JOURNAL OF MATERIALS PROCESSING TECHNOLOGY 209 (2009) 2648–2661

journal homepage: www.elsevier.com/locate/jmatprotec

Multi-stage metal forming: Variation and transformation

J. Post[a,*], *G. Klaseboer*[a], *E. Stinstra*[b], *T. van Amstel*[a], *J. Huetink*[c]

[a] *Philips DAP B.V., Advanced Technology Building AX-24, P.O. Box 20100, Oliemolenstraat, 5, 9200 CA Drachten, The Netherlands*
[b] *CQM, P.O. Box 20100, 9200 CA Eindhoven, The Netherlands*
[c] *University of Twente, Drienerlolaan 5, 7522 NB Enschede, The Netherlands*

ARTICLE INFO

Article history:
Received 6 December 2007
Received in revised form
22 May 2008
Accepted 8 June 2008

Keywords:
DACE
Distributed computing
FEM
Stainless steel

ABSTRACT

During precision forming of metal parts made of metastable austenitic stainless steels, the relationship between the scatter on the initial parameters like the strip thickness, yield stress, etc. on the product accuracy need to be known. This becomes complex if the material is instable, i.e. martensite forms very easily. The transformation rate depends on the stress state, which is related to friction. It also depends on the temperature, which is related to deformation heat. A greater understanding of these phenomena is obtained by doing a process window study, using design and analysis of computer experiments (DACE). This paper demonstrates how to perform a DACE study on a three-stage metal forming process, using distributed computing. The study focuses on:

- Hardening due to strain-induced and stress-assisted transformation.
- The influence of metal forming parameters on the product accuracy.

1. Introduction

Metastable austenites may transform to martensite during or after metal forming. These transformations depend on temperature and hydrostatic stress, which make the constitutive model complex and difficult to implement. The calculations described in this article have therefore been executed with a dedicated and robust internal Philips FEM solver called CRYSTAL. Because of the influence of temperature, the calculations need to be fully thermo-mechanically coupled. The calculations also have to incorporate the effects of friction, because it influences the stress state. This code has been specifically developed to describe multi-stage metal forming processes including complex materials behaviour. The material used for these calculations is a corrosion-resistant steel, referred to as Sandvik Nanoflex™ (Holmquist et al., 1995).

Developing and implementing a multi-stage process, including heat treatments is a very complex task. There are a number of issues to consider:

(1) Development of metal forming processes is normally done in an empirical way, especially multi-stage processing. The combination of a complex multi-stage process with a very complex material will lead to long development times.
(2) Process robustness is an important issue for this kind of processes. Chemical composition has an influence on the stability of the austenite. To carry this out in an empirical way is a very costly and time-consuming proposition

* *Corresponding author*. Tel.: +31 512 594454.
E-mail addresses: j.post@philips.com (J. Post), e.stinstra@cqm.nl (E. Stinstra), j.huetink@ctw.utwente.nl (J. Huetink).
URL: http://pww.nl/dap/philips.com/atc (J. Post).

0924-0136/$ – see front matter © 2008 Elsevier B.V. All rights reserved.
doi:10.1016/j.jmatprotec.2008.06.061

because one has to make a number of different melts with different compositions.

So in general, it can be said that developing multi-stage processes in combination with metastable stainless steels is a complex and time-consuming affair. This approach speeds up the development very much.

2. The material model for Sandvik Nanoflex™

2.1. Introduction

Sandvik Nanoflex™ belongs to the category of metastable austenitic stainless steels. It is also a precipitation hardenable steel, which means that the martensite phase can be aged (Holmquist et al., 1995; Narutani et al., 1982). For the chemical composition (see Table 1).

Depending on the stability of the steel, two phenomena occur:

(1) A stress-assisted transformation, below the flow stress of the composite.
(2) A strain-induced transformation, above the flow stress of the composite at higher temperatures above the martensite start temperature M_s^σ.

These transformations are stress-state and temperature dependent.

A general differential equation for the transformation behaviour was constructed:

$$\varphi = c(D+\varphi)^{n_a}(f_s-\varphi)^{n_b} \quad (1)$$

where φ is the martensite content, c related to the mean transformation rate, D related to the nucleation or initial transformation rate, f_s the saturation value of the transformation and n_a and n_b are fit constants that determine the shape of the curve. The first part of the equation $(D+\varphi)^{n_a}$ describes how the transformation rate increases because the formed martensite has a bigger volume, which causes stresses in these regions. If the hydrostatic part of the stress is positive, it accelerates the transformation. When most of the material has transformed, the transformation rate decreases. The local hydrostatic stress becomes negative in the retained austenite. Depending on the kinetics, the transformation will stop. This is described by the last term of Eq. (1): $(f_s-\varphi)^{n_b}$

The martensite transformation is split into two parts:

(a) One below the yield stress of the composite, the stress-assisted transformation.
(b) One at and above the yield stress of the composite, the strain-induced transformation.

The total martensite content is the summation of both these types of transformation:

$$\varphi = \varphi_{strain} + \varphi_{stress} \quad (2)$$

The kinetics of the strain-induced martensite transformation depends only on the amount of plastic energy generated during the deformation.

2.2. Strain-induced transformation

Eq. (1) was adapted to apply to the strain-induced transformation:

$$\varphi_{strain} = C_{strain}(T,\sigma^H,Z)[(D_1+\varphi)^{n_1}(f_{strain}-\varphi)^{n_2}]\varepsilon^p \quad (3)$$

where φ is the martensite content, f_{strain} is the saturation level of transformation and C_{strain} is a function that describes the dependence of the transformation on the temperature, hydrostatic stress and the structure of the material. Z is a parameter that depends on the annealing conditions before metal forming, the chemical composition and the crystal orientation, see Figs. 1 and 2. C_{strain} is related to the thermodynamics of the transformation. The following function is assumed based on curve fitting:

$$C_{strain} = Q_1(1+Q_2\tanh(Q_3\sigma^H))(e^{(T-T_0)^2/Q_4}-Q_5) \quad (4)$$

Here Q_1 is a constant describing the mean transformation rate; Q_2, Q_3 describe the influence of the stress state and Q_4, Q_5 describe the influence of the temperature on the transformation and T_0 is the temperature of the nose of the TTT-diagram. The influence of the chemical composition and the crystal orientation is neglected. The values of Q, n_2 and T_0 can be found in Table 2.

2.3. Stress-assisted transformation

The following equation was used to describe the stress-assisted transformation based on Eq. (1).

$$\varphi_{stress} = C_{stress}(T,\sigma^H,\varepsilon^p,Z)[(D_2+\varphi)^{n_3}(f_{stress}(T,\sigma^H,Z)^{n_4}] \quad (5)$$

where C_{stress} is a function that describes the dependence of transformation on stress, temperature and material structure. D_2 is a constant.

$$C_{stress}(T,\sigma^H,\varepsilon^p) = C^1_{stress}(T)C^2_{stress}(\sigma^H)C^3_{stress}(\varepsilon^p) \quad (6)$$

$$f_{stress}(T,\sigma^H,\varepsilon^p) = f^1_{stress}(T)f^2_{stress}(\sigma^H)f^3_{stress}(\varepsilon^p) \quad (7)$$

Table 1 – Chemical Composition of Sandvik NanoFlex™

Element	wt%
C, N	<0.05
Cr	12
Ni	9
Mo	4
Ti	0.9
Al	0.3
Si	0.15
Cu	2.0

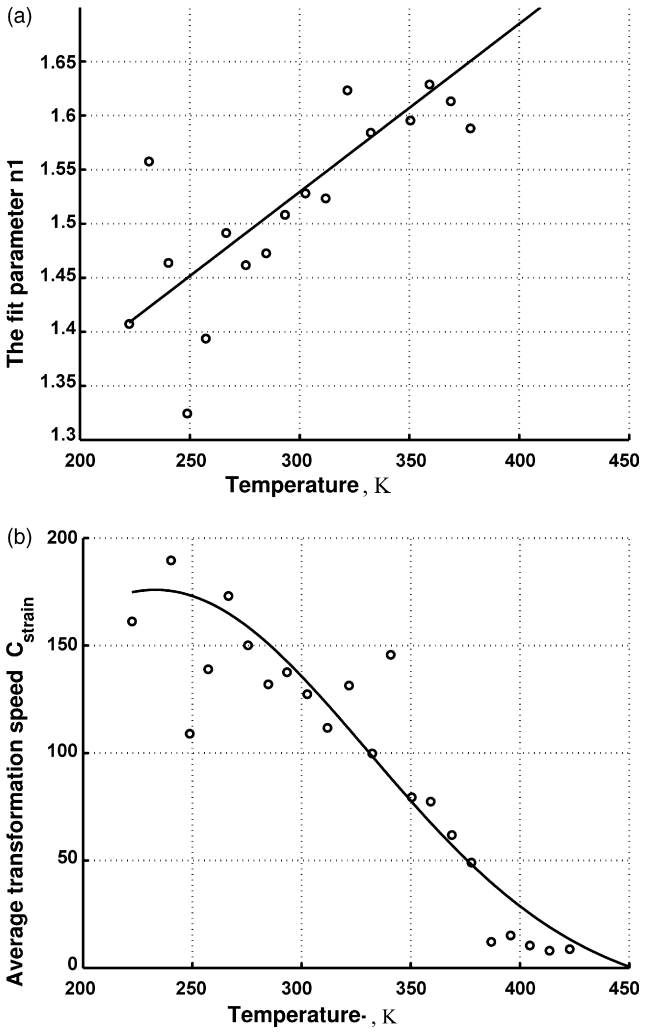

Fig. 1 – (a) The fit parameter n_1. See Table 2 for the other fitted parameters. (b) The temperature dependence of the strain-induced transformation C_{strain}.

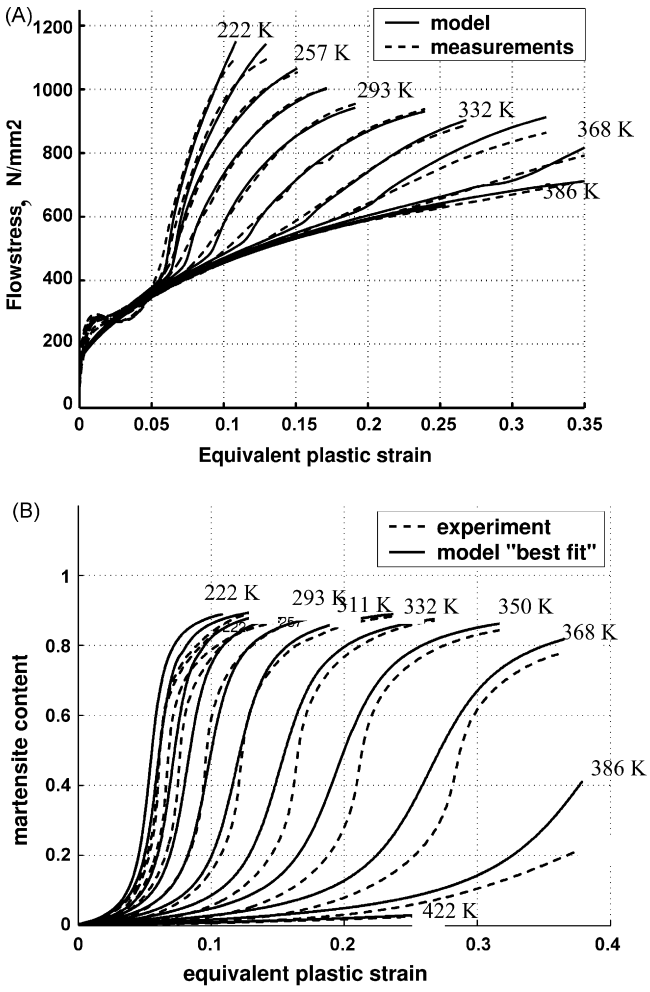

Fig. 2 – The fitted model and measured data. Right: the strain-induced martensite. Left: the flow stress. In the both figures, the lines furthest to the left correspond to a temperature of 223 K whereas the lines furthest to the right correspond to 423 K (increment ±20 K).

Table 2 – Value of the fitted parameters for the flow stress and the strain-induced transformation

Q_1	184	Q_2	0.50
Q_4	14,629	Q_5	0.056412
$\sigma_{0\gamma}$	175.8 (N/mm^2)	$\sigma_{0\alpha}$	694.2 (N/mm^2)
m_γ	1087	m_α	140
n_1	1.108 + 1.3624E−3T	b	2
C_1	12.477	C_2	22.822
C_4	$-1.0267 + 1.3282\dot{\varepsilon} + 0.020436T$	C_5	62.268
C_7	1.7934	C_8	$0.54154 - 0.46797\dot{\varepsilon} - 0.7171E-4T$
C_{10}	1.8961	φ_γ	1.9061E−4
Q_3	0.005	f	0.95
φ_0	0.7981 + 1.278E−4T	q	0.24 + 3.1079E−4T
C_3	0.61054	D_1	9.7259E−3
n_2	2	D_2	0.13
C_6	2.7907	C_9	$0.8062\exp(-(T-196)^2/7457.3)$
φ_α	− 9.78E−4	T_0	223 K

The following relations for C_{stress}, D_2 and f_{stress} are proposed, where $R_1 \ldots R_{17}$ are constants, based on fitting.

$$C^1_{stress}(T) = R_1 \ \exp\left(\frac{-(T-232)^2}{R_2}\right) \quad (8)$$

$$C^2_{stress}(\sigma^H) = R_3 + \left[\frac{1}{2} + \frac{1}{2}\ \tanh(R_4(\sigma^H - R_5))\right](1-R_3) \quad (9)$$

$$C^3_{stress}(\varepsilon^P) = R_6 + \left[\frac{1}{2} + \frac{1}{2}\ \tanh(R_7(\varepsilon^P - R_8))\right](1-R_6) \quad (10)$$

$$f^1_{stress}(T) = R_{10}\ \exp\left(\frac{-(T-232)^2}{R_{11}}\right)(1-R_{10}) \quad (11)$$

$$f^2_{stress}(\sigma^H) = R_{12} + \left[\frac{1}{2} + \frac{1}{2}\ \tanh(R_{13}(\sigma^H - R_{14}))\right](1-R_{12}) \quad (12)$$

$$f^3_{stress}(\varepsilon^P) = R_{15} + \left[\frac{1}{2} + \frac{1}{2}\ \tanh(R_{16}(\varepsilon^P - R_{17}))\right](1-R_{15}) \quad (13)$$

The fit resulted in the parameters that are presented in Tables 3 and 4. Some of the results from the model are shown in Fig. 3. This model provides a good prediction of the saturation value of the martensite content, especially for the unstable material.

Two distinct austenitising conditions were used.

A stable treatment, from now on referred to as pre-treatment 1. The material was austenitised at 1323 K for 30 s and then slowly cooled to room temperature (quenching with 1 bar recirculating inert gas). This treatment took place in a vacuum furnace.

An unstable treatment, from now on referred to as pre-treatment 2. The material was austenitised at 1323 K for 15 min and then cooled down quickly to room temperature (quenching with 6 bar recirculating inert gas). This treatment took place in a vacuum furnace.

2.4. *Path dependent dislocation based on work hardening*

For this study it is assumed that the work hardening depends on plastic strain, martensite content, temperature, and plastic strain rate. The model used is founded on the physically based models of Estrin (Estrin, 1996), describing dislocation densities as internal state variables. The work hardening mechanism is not only based on change in dislocation density but also on other structural defects such as subgrains, etc. Therefore, parameter Y is not the dislocation density alone but the resistance of dislocation movement caused by structural defects in relation to plastic deformation. In this study only one dislocation density was used for each phase. The original model was modified to make it as simple as possible and reduce the number of unknowns. For the flow stress of austenite, we assumed:

$$\sigma^Y_\gamma = \sigma_{0\gamma}\sqrt{Y_\gamma}\left(1 + \frac{\varepsilon_P}{\psi_\gamma}\right)^{1/m_\gamma} \quad (14)$$

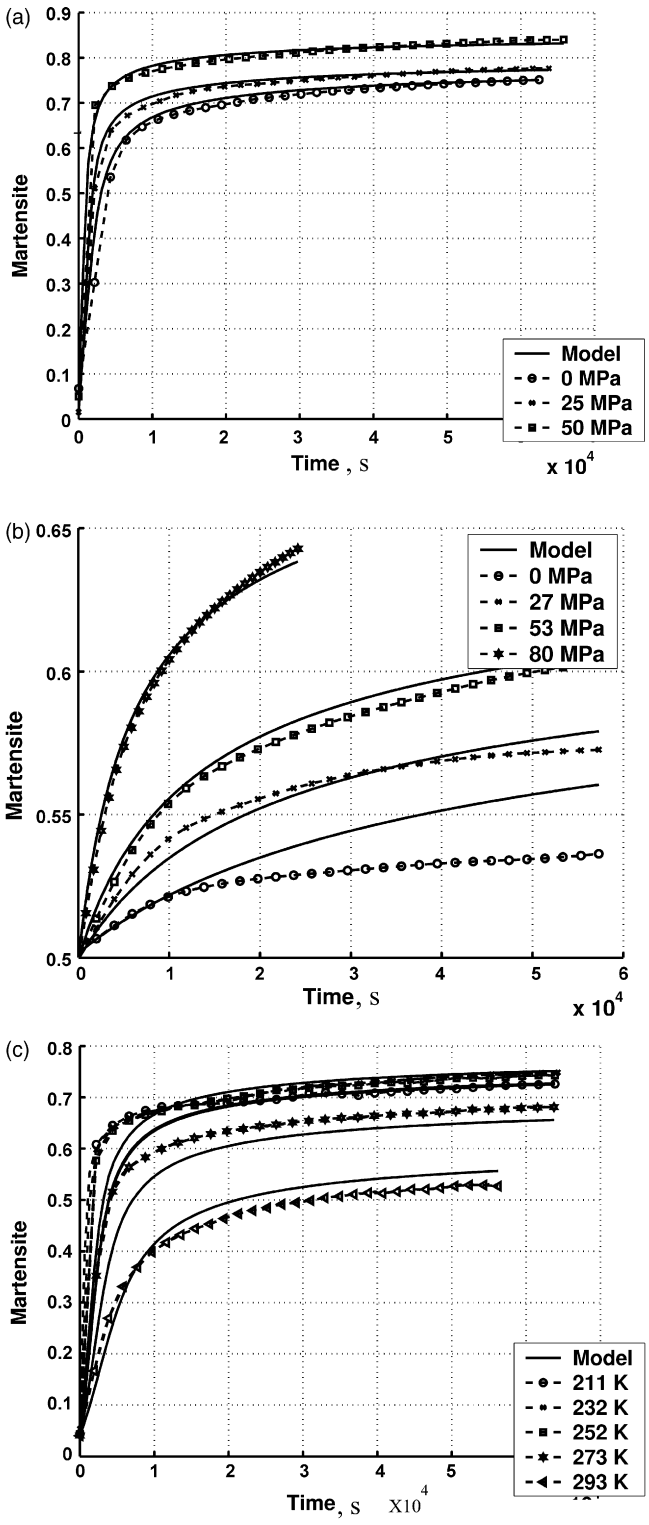

Fig. 3 – The stress-assisted transformation. (a) The influence of the applied stress on the stress-assisted transformation of unstable material. (b) The influence of the hydrostatic stress on the stress-assisted transformation, of stable material (pre-treatment 1) after deforming the specimen until the strain-induced martensite reaches 0.5. (c) Temperature dependence of the transformation of unstable material (pre-treatment 2).

Table 3 – Value of the fitted parameters for stable material

R_1	1.2E−1	R_2	2.8E3	R_3	0	R_4	2.4E−3 (N/mm^2)
R_5	4.2E−3	R_6	19.6	R_7	4.4	R_8	3.0E−2
R_9	1.3E−1	R_{10}	−2.0	R_{11}	8.9E4	R_{12}	6.2E−1
R_{13}	1.6E−2	R_{14}	0	R_{15}	0	R_{16}	20
R_{17}	2.5E−2	n_3	2.9	n_4	6.0		

And for the flow stress of martensite,

$$\sigma_\alpha^Y = \sigma_{0\alpha}\sqrt{Y_\alpha}\left(1+\frac{\varepsilon_P}{\psi_\alpha}\right)^{1/m_\alpha} \tag{15}$$

Value 1 was implemented in Eqs. (14) and (15) in order to avoid a high derivative of $d\sigma/dt$ at low strain rates, and to avoid the problem that the flowstress becomes zero when there is no plastic strain. For example, at the beginning of plastic deformation, this condition leads to problems in the stiffness matrix in a FEM solver. In these equations, σ_0 is the basic stress that depends on strain rate and temperature, φ represents the martensite content, Y the general dislocation density for one phase, ε^p is the equivalent plastic strain rate, $\psi_{\alpha,\gamma}$, the reference strain rate and $m_{\alpha,\gamma}$, are constants that depend linearly on strain rate and temperature for this study. The metal consists of both the austenite and the martensite phases. Thus, when both these phases are combined, the equation becomes:

$$\sigma^Y = \sigma_\gamma^Y - \frac{1}{2}\left[1+\tanh\left(\frac{\varphi-\varphi_0}{q}\right)\right](\sigma_\alpha^Y - \sigma_\gamma^Y) \tag{16}$$

The constants φ_0, q were introduced to describe the nonlinear relation between the flow stresses as a rule of mixture. At low martensite contents, the influence of martensite will be lower than at high levels of martensite. The evolution of the dislocation density in the austenite is described as follows:

$$\begin{aligned}\dot{Y}_\gamma &= [C_1(C_2 - Y_\gamma)^{C_3} + C_4(\dot{\varepsilon}_P, T)]\dot{\varepsilon}_P \\ \dot{Y}_\gamma &= [C_4(\dot{\varepsilon}_P, T)]\,\dot{\varepsilon}_P \quad \text{if} \quad Y_\gamma > C_2\end{aligned} \tag{17}$$

where C_1, C_2, C_3 are material constants and C_4 depends on temperature and strain rate. The constants are not directly related to physical phenomena but are chosen to fit the model.

In a similar way, the following equation applies to the dislocation density in the martensite phase:

$$\begin{aligned}\dot{Y}_{\alpha_1} &= [C_5(C_6 - Y_\gamma)^{C_7} + C_8(\dot{\varepsilon}_P, T)]\dot{\varepsilon}_P \\ \dot{Y}_{\alpha_1} &= [C_8(\dot{\varepsilon}_P, T)]\,\dot{\varepsilon}_P, \quad \text{if} \quad Y_\alpha > C_6\end{aligned} \tag{18}$$

where C_5, C_6, C_7 are material constants and C_8 depends on temperature and strain rate.

During transformation, three different phenomena occur:

- recovery of the dislocations takes place due to generation of virgin martensite;
- the dislocations in the austenite are not annihilated during the transformation but are partly transferred to the martensite;
- new dislocations are formed at the transformation boundary.

The second effect depends on the temperature. Suppose we start with a volume V having a specific amount of martensite φ and a dislocation density of Y_α. After a deformation step, the martensite content is increased by $d\varphi$ and the dislocation density is increased by dY_α. This means

$$(\varphi + d\varphi)(Y_\alpha + dY_\alpha) = \varphi Y_\alpha + C_9(T)\,d\varphi\;\; Y_\gamma + d\varphi C_{10} \tag{19}$$

where φY_α is the initial dislocation density, C_9 is the parameter, which describes the inheritance of dislocations from austenite to martensite and C_{10} represents the generation of dislocations on the transformation boundary. It is assumed that at this temperature, C_9 will reach its maximum. From Eq. (19) it follows:

$$C_9(T)\,d\varphi\;\; Y_\gamma + C_{10}\,d\varphi = d\varphi\,Y_\alpha + d\varphi\,Y_\alpha \tag{20}$$

or

$$\dot{Y}_\alpha = \frac{\dot{\varphi}}{\varphi}(C_9(T)Y_\gamma + C_{10} - Y_\alpha) \tag{21}$$

Here $\dot{\varphi}/\varphi\,(C_9(T))$ is the dislocation inheritance of the dislocation density, $\dot{\varphi}/\varphi\,(C_{10})$ represents the generation of new dislocations on the transformation $-\dot{\varphi}/\varphi\,(Y_\alpha)$ boundary and is the recovery due to new, virgin martensite.

It is assumed that the generation of dislocation density on the boundary is much higher with lath martensite, resulting from the strain-induced transformation, than with plate martensite, resulting from the stress-assisted transformation. This means that the generation of dislocations on the boundaries is related only to the φ_{strain}, and the inheritance and recovery effects are related to the total martensite content. We have to split Eq. (21) into two parts, one related to the total transformation rate and one related to the strain-induced

Table 4 – Value of the fitted parameters for instable material

R_1	1.2E−1	R_2	2.8E3	R_3	−4.6E−4	R_4	2.46E−3 (N/mm^2)
R_5	4.2E−3	R_6	2.6	R_7	4.4	R_8	3.0E−2
R_9	1.5E−1	R_{10}	−2.0	R_{11}	8.9E4	R_{12}	7.5E−1
R_{13}	1.6E−2	R_{14}	65	R_{15}	l.2	R_{16}	20
R_{17}	2.5E−2	n_3	2.9	n_4	6.0		

transformation rate:

$$\dot{Y}_{\alpha_2} = \frac{-\dot{\varphi}_{\text{strain}}}{\varphi}(C_9(T)Y_\gamma + Y_\alpha) \tag{22}$$

where C_9 is a constant that depends on the temperature. The values of C_9 are calculated by curve fitting.

For the generation of dislocations on the transformation boundary, the following equation is introduced.

$$\dot{Y}_{\alpha_3} = \frac{-\dot{\varphi}}{\varphi}C_{10} \tag{23}$$

where C_{10} is a constant.

From Eqs. (18), (22) and (23) the following equation is defined for the dislocation density in the martensite phase:

$$\dot{Y}_\alpha = \dot{Y}_{\alpha_1} + \dot{Y}_{\alpha_2} + \dot{Y}_{\alpha_3} \tag{24}$$

The model developed this way is finally used to calculate the stress and fraction of martensite formed as a function of strain, strain rate and temperature. A comparison between the measured and the calculated stress–strain curves are shown in Fig. 2. For more information on the material model, refer to Post et al. (2008).

3. Three-stage metal-forming process

3.1. Introduction

The main purpose for developing the material model for Sandvik Nanoflex™ is applications in simulations on multi-stage metal forming processes. These kind of processes are normally used for mass production of metal parts, using progressive tooling. To validate the model and its robustness, a multi-stage process is defined, consisting of three different steps. The calculations are carried out together with experiments.

The example product is a combination of a spring and a bearing. The contact area of the bearing is the radius on the top of the product (Fig. 5). This radius part of the product must have a specific hardness (Hv) to avoid wear during operation. The other dimensions of the product are related to a specific stiffness in the vertical direction in order to facilitate clamping.

The total production process consist of the following steps, see also Fig. 4:

(1) A stamping step, a simple deep drawing operation.
(2) A waiting step which simulates the transport of the product from stamping step 1 to 2.

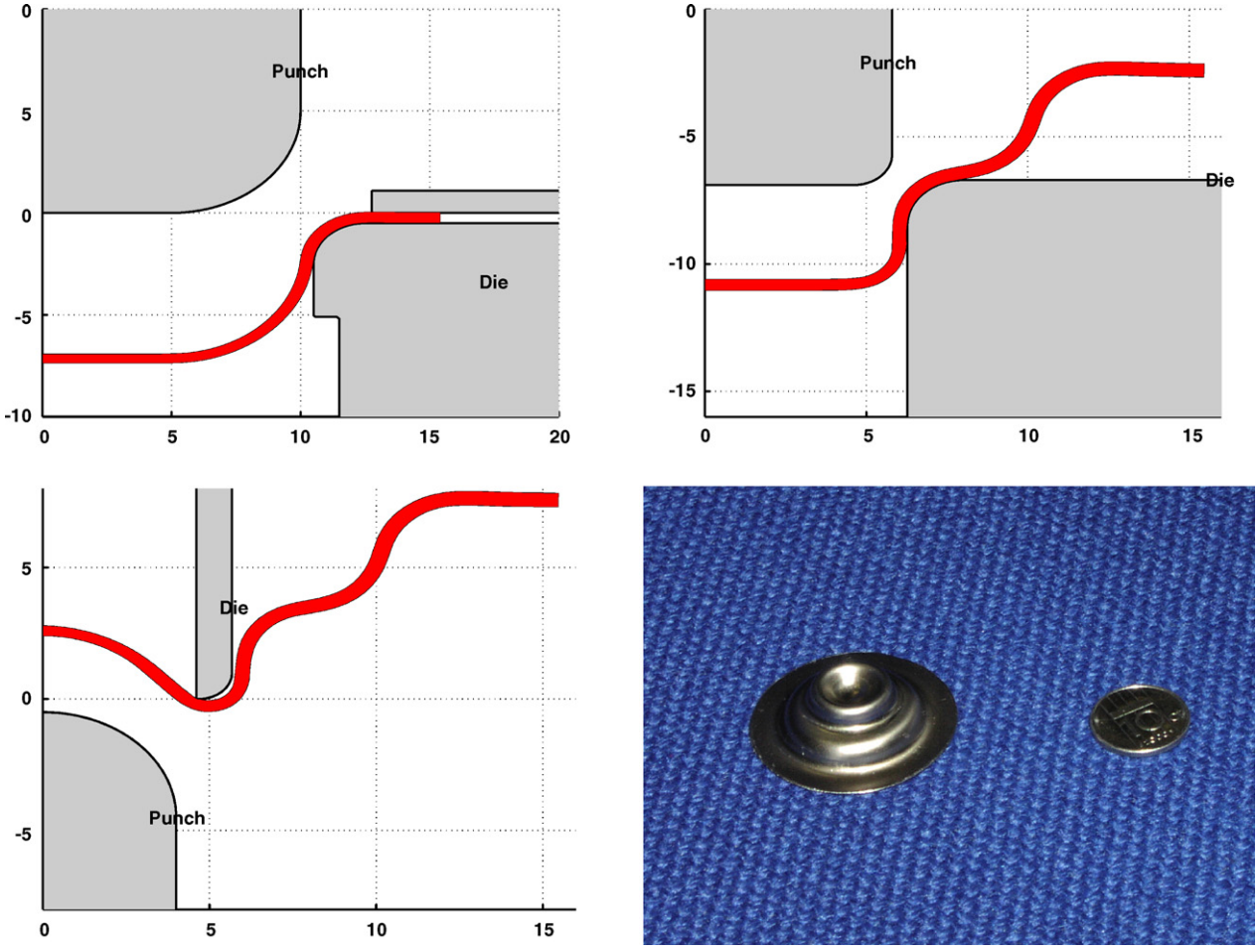

Fig. 4 – The example process. Top left: step 1; top right: step 2; bottom left: step 3. Dimensions in mm. Bottom right: photograph of the product. All cross-sections were made at the end of the process.

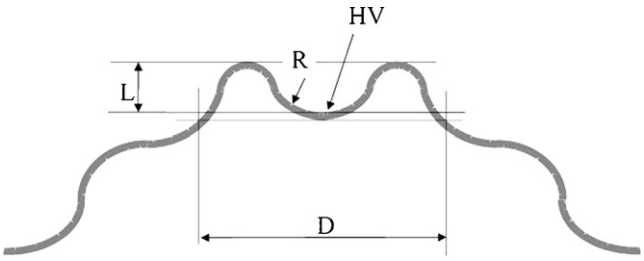

Fig. 5 – A sketch of the example product.

(3) A stamping step, the second deep drawing step.
(4) A waiting step, simulating the transport from stage 2 to stage 3.
(5) A stamping step: biaxial stretching in the reverse direction.
(6) A waiting step, this is the time from stamping up to austenitising.
(7) Austenitising for 15 min on 1323 K, quenching using 6 bar recirculating inert gas: during this time step the material becomes unstable.
(8) An isothermal transformation step at 223 K for 24 h.
(9) A precipitation step 15 min at 773 K.

During the stamping process the product becomes partly martensitic, during waiting, this transformation continues. After autenitising the product is fully austenitic and during isothermal transformation it becomes martensitic again at a level of about 60–80%. During this transformation, plasticity and dilation strain occur, resulting in dimensional changes of the product.

3.2. *Implementation in the FEM code*

All the functions mentioned above were implemented in a dedicated metal forming code called crystal defining three different models:

- One for stamping and waiting of stable material.
- One for austenitising.
- One for the transformation of instable material.

All the calculations were fully thermo-mechanically coupled and the effects of friction were included because they influence the stress state. The tools were described as rigid bodies. The material properties after a calculation step were mapped on to the model for the next step to incorporate the cumulative effect of the transformation and work hardening during the different steps.

3.3. *FEM simulations and verification*

Fig. 6 shows the results of the calculations after the different metal forming steps and waiting steps. In addition, the process was validated after steps 2, 4 and 6 using an automatic measuring method based on image processing (Post et al., 2001). The product contours and martensite profile were measured.

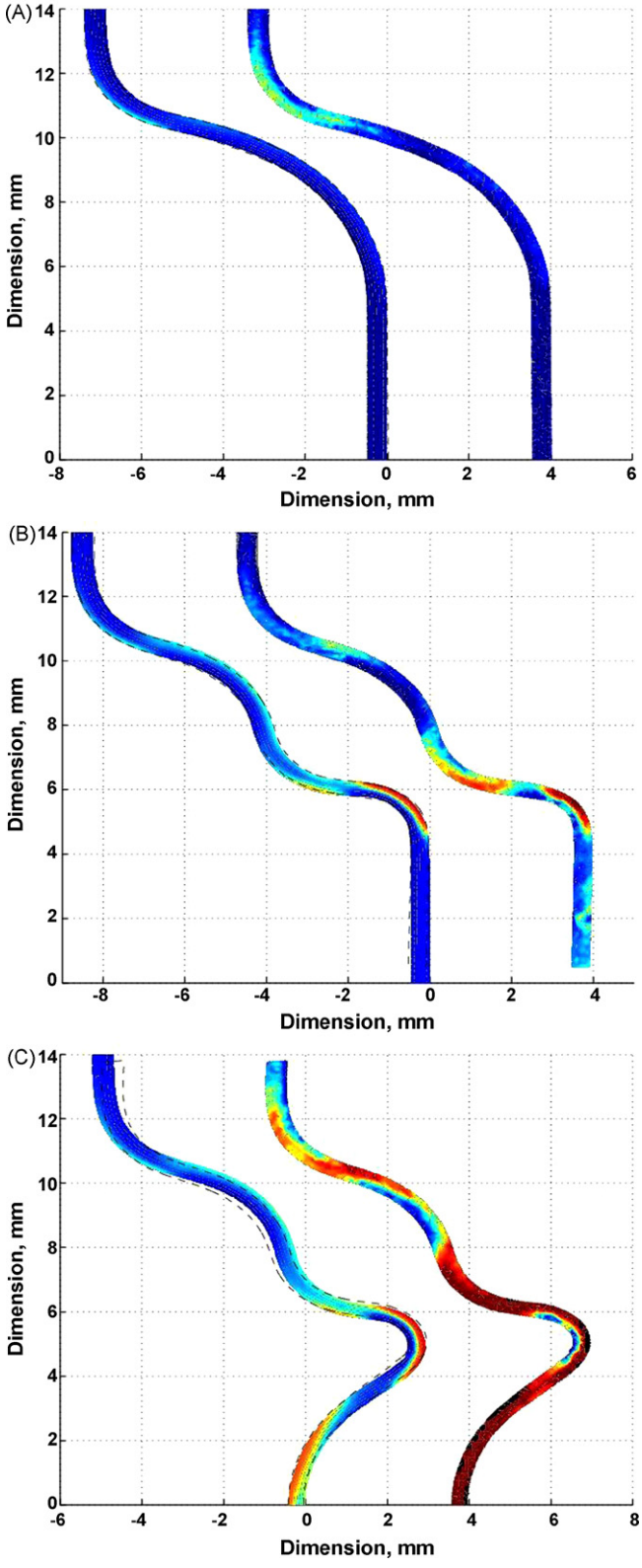

Fig. 6 – The example process. In the figures, the contours on the right are the calculated products, the ones on the left are the measurements. Martensite is represented in red ans austenite in blue.

4. Process window studies: design and analysis of computer experiments (DACE)

4.1. Motivation

There are a number of reasons for using the DACE approach in this study:

(1) One simulation of the total process takes more than 1 day; this makes it very difficult and time consuming to implement a calculation like this directly in an optimization scheme. It is much more effective to do it indirectly with is done with the DACE approach.
(2) The difference between design of experiments (DOE) and DACE lays in the fact the repeating a empirical test will create different result while repeating a calculation will create the same result. This means that the standard deviation of the sample size of calculations is zero and as a result you need only one calculation and not a number of them to predict the mean of a sample size.
(3) The DACE approach is commercial available as a software package called COMPACT.
(4) The DACE approach is universal. This means that this approach can be used for every optimization problem, only the applications are different.

4.2. Introduction

The ever-increasing pressure on the development time of new products and processes has changed the design process during recent years. In the past, design merely consisted of experimentation and physical prototyping. In the last decade, computer simulation models such as FEM and CFD have become very popular in engineering design and analysis. The application described in this part is one of many examples. In many cases, only predicting the quality characteristics of a design is not enough. Usually, designers are confronted with the problem of finding settings for a number of design parameters that are optimal with respect to several product or process quality characteristics (see Table 5). Since there are usually many possible combinations of design parameter settings, the crucial question becomes how to find the best possible settings with a minimum number of simulations. This new challenge has led to a new engineering discipline, often referred to as DACE. Surveys on this research area can be found in (Myers, 1999; Barthelemy and Haftka, 1993). All methodologies that are suggested in the literature rely heavily on statistics and mathematical optimization theory. Generally, there are two types of approaches: iterative approaches (Bakircioglo and Kocak, 2000) and global modelling approaches (Booker et al., 1999). Many papers have been published on applications of DACE in a wide variety of engineering disciplines. In this part, the DACE method 'Compact' and its application on optimizing the manufacturing process is presented. 'Compact' has already been used in several cases (Hertog den and Stehouwer, 2002), and is based on global modelling.

4.2.1. Methodology and application

In this section, the 'Compact' methodology is presented. The approach consists of four steps: problem specification, design of computer experiments, 'Compact' modelling and analysis. Fig. 7 gives an overview of the steps. Along with these steps, the implementation is described in the previous section.

4.2.2. Problem specification

In the first step, the design optimization problem is defined. First of all, the definition is needed for the design parameters that are varied. Generally, two types of design parameters can be distinguished:

- Parameters for which the optimal settings with respect to the quality characteristics have to be found.
- Parameters that have significant influence on the quality of the design, which cannot (completely) be controlled in the physical reality. In this case all the design variables of interest fall into the second category: we cannot control the design parameters (see Table 5). The objective in this case was not to find the optimum setting of design variables but to gain insight into the robustness of several quality characteristics. Next, definition is required of the quality characteristics that are important in evaluating the design. These quality characteristics are usually referred to as response parameters. In this case, response parameters

Table 5 – The input parameters for the DACE analyses

Parameter	High	Low	Dimension	Distribution	S
Initial temperature	288	298	K	n	5
Material thickness	0.49	0.5	mm	n	0.01
Influence chemical composition (C_{strain})	280	420	K	n	25
Initial flow stress austenite	280	380	N/mm^2	n	50
Saturation value for martensite (f_{stress})	0.6	0.8	–	n	0.1
Time step between step l and step 2	0	600	s	u	300
Time step between step 2 and step 3	0	600	s	u	300
Waiting time after step 3	100	10,800	s	u	5350
Ram depth step l related to nominal	−0.02	+0.02	mm	n	0.02
Ram depth step 2 related to nominal	−0.02	+0.02	mm	n	0.02
Ram depth step 3 related to nominal	−0.02	+0.02	mm	n	0.02
Coulomb friction	0.008	0.15	–	n	0.035

Distribution: n = normal; u = uniform; S = standard deviation.

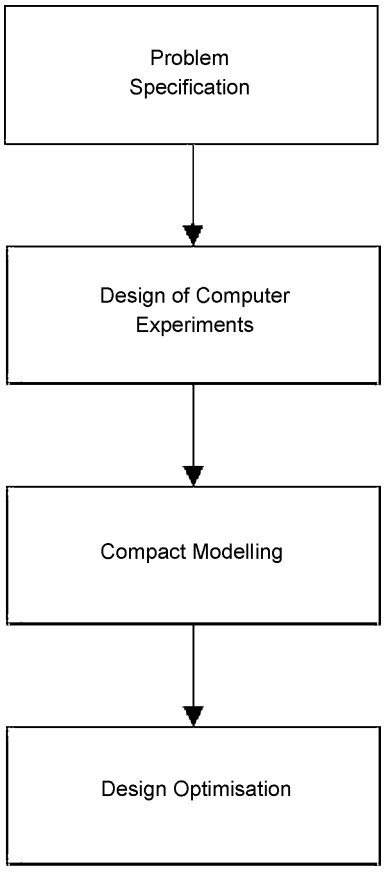

Fig. 7 – 'Compact' approach.

are divided into three process steps. For every step, the response parameters are printed in Table 6.

4.2.3. *Design of computer experiments*

The second step in the 'Compact' methodology generates a set of suitably chosen combinations of design parameter settings or design points that must be located within the feasible design region, i.e., the part of the design parameter space that satisfies all bounds on the design parameters defined in step 1. The problem of choosing the design points is called Design of Experiments (DOE) (Montgomery, 1984). Classical DOE mainly focuses on physical experimentation in which experiments are subject to noise as opposed to computer experiments in which the same calculation will always give the same results. Therefore, classical DOE schemes have a number of drawbacks when used for computer experimentation. In computer experimentation, a DOE should be:

Table 6 – Dimensions and tolerances of the example process

Symbol	Name	Nominal	Tolerance
D	Diameter	13 mm	±0.01 mm
L	Bearing high	3 mm	±0.01 mm
R	Bearing radius	4.06 mm	±0.005 mm
Hv	Bearing hardness	500 Hv0.2	±50 Hv0.2

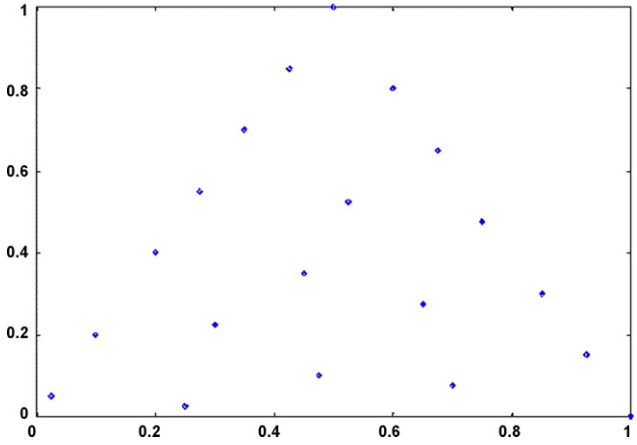

Fig. 8 – Computer-generated space-filling LHD.

- Space-filling, i.e. the minimal distance between any two design points should be a maximum. Compared to classical DOE, this means that design points will also be located in the interior of the feasible design space.
- Non-collapsing, i.e. when all design points are projected on to one (any) (design parameter) dimension, no two design point projections should be equal.
- Able to deal with non-box and integrality constraints: this means that the whole design matrix does not necessarily have to be filled with data.
- Expandable, i.e. it should be possible to add design points that comply with above-mentioned criteria.

The approach used in 'Compact' satisfies all of the these criteria. It searches for the best space-filling simulation scheme within the class of so-called latin hypercube designs (LHD) using a simulated annealing algorithm (Aarts and Korst, 1989). Fig. 8 gives an example of a constrained 2D simulation scheme generated by 'Compact' (see Hertog den and Stehouwer, 2002 for a more elaborate discussion on the 'Compact' LHD module). In the case described in Section 3, a scheme was constructed consisting of 120 design points. Since simulation of one design point takes approximately 24 h, all design points were simulated using distributed computing (taking a total calculation time of 3000 h). See Section 4 for details on the distributed computing technique used.

4.2.4. *'Compact' modeling*

The third step in the 'Compact' methodology consists of fitting a 'Compact' model for every response parameter in terms of the design parameters. The models are based on the simulation output generated after step 2. Other frequently used terms for 'Compact' models include: 'approximating model', 'Response Surface Model (RSM)' and 'meta-model'. For the purpose of predicting the results of a computer model, second order polynomial models, Kriging models (Sacks et al., 1989) and Neural Networks (Bakircioglo and Kocak, 2000) are frequently used. The 'Compact' approach supports both polynomial models (using a step-wise term selection technique) and Kriging models. The first type is preferred, as Kriging models are more time-consuming to fit and harder to

Table 7 – Relative importance of the first 10 coefficients in the polynomial 'Compact' model for the radius after metal forming and waiting

Coefficient	Influence
Material thickness × friction	0.043
Friction	0.031
Initial flowstress	0.030
Time 2 –>3 × Time 2 –>3	0.018
Material thickness × Material thickness	30.016
Initial temperature × Depthstep 2	0.016
Material thickness × Initial flowstress	0.015
Depthstep l × Depthstep 1	0.014
Depthstep 3	0.013

These data are constructed using the intervals of the parameters from Table 5 (high–low) in combination with a second-order normalized model, including the possible interactions.

validate. Kriging may be necessary though, when the physics becomes so non-linear that a polynomial model of moderate degree cannot fit the data. Validation of the model is of course of great importance. There are several statistics that can be used for this purpose. Amongst these are, e.g. RMSE, cross-validation RMSE and the error on an independent test set. For more information on model validation, see Conn et al. (2000). When a model is not accurate enough, two options exist. First, the design space can be decreased and a better model can be sought for this new region. This may imply that new simulations are needed in the new design space. Second, design points can be added to the original design space, simulated, and fitted to a new model. Eventually, this procedure will lead to an accurate 'Compact' model. In the case described in Section 3, five 'Compact' models were fitted. As an example, the validation results based on step-wise second order polynomial models are presented in Table 7.

4.2.5. *Analysis*

Steps 1 to 3 result in a 'Compact' model for each of the response parameters.

In step 4, these models are exploited by four types of analysis:

- Prediction: since the 'Compact' models can be evaluated very quickly compared to a simulation run, prediction using a 'Compact' model is much more attractive.

What-if scenario analysis can be performed by just changing a design parameter and evaluating 'Compact' models;

- Optimization: since prediction can be performed so quickly, traditional optimization techniques that usually require many function evaluations become feasible. In step 1, the feasibility of the designs is defined and the preferability of the given design above another is determined using an objective function. These definitions can be exploited and the globally optimum design can be found using global Mixed Integer Non-Linear Programming (MINLP) techniques.
- Robust design: in step 1 it is determined which design parameters are controllable in reality and which are not. By defining a random distribution for each of the non-controllable design parameters, a Monte Carlo analysis is performed and the robustness of a design is evaluated.
- Sensitivity analysis: usually, more than one conflicting objective exists. Using 'Compact' models and optimization techniques, it is easy to create a curve indicating all Pareto optimum designs.

In this case the robust design module was used to evaluate the spread of product characteristics in relation to the spread on the design parameters:

- Influence on the product accuracy of two types of hardening (strain-induced and stress-assisted).
- The influence of metal forming parameters on the form accuracy and the hardness.

4.3. *Case studies*

4.3.1. *Introduction*

4.3.1.1. Case 1: hardening and accuracy. There are two possibilities to harden a product made from Sandvik Nanoilex™:

(1) Using the strain-induced transformation.
(2) Using the stress-assisted transformation.

It is interesting to compare the two. Hence, different Monte Carlo calculations were carried out to study the hardness after ageing and the accuracy of the example product. The results of three Monte Carlo simulations are shown in the following figures:

- Fig. 9A and B give the results directly after stamping.
- Fig. 9C and D give the results after stamping and waiting for 10,800 s. It is assumed that after this time the stress-assisted transformation has stopped as the positive residual stress vanishes, because of the dilation strain. The results are very similar to that after stamping but there are some small dimensional changes.
- Fig. 9E and F give the results after stamping, waiting, re-austenising and isothermal hardening. The graphs show that using this method the hardness increases, but the accuracy of the radius decreases. This is related to the dilation strain, and transformation plasticity.

4.3.1.2. Case 2: the influence of metal forming parameters on the form accuracy and the hardness. A second Monte Carlo analysis was carried out on the product. The results for the hardness and the radius are shown in Fig. 10A and B. It can be seen that the expected hardness was 462.7 Hv with a standard deviation of 15.6 Hv. The radius was 4.068 mm with a standard deviation of 5.7 μm. The goal of the research was to investigate the influence of waiting time on the form accuracy and the hardness. Hence a Monte Carlo analysis is carried out with the nominal values from Table 6, only the waiting times were varied. Note that the interactions between waiting times and other variations are excluded this way. The results are shown in Fig. 10C and D. From these results it can be concluded that the waiting times between the different steps do have an influence but are not the main factor for

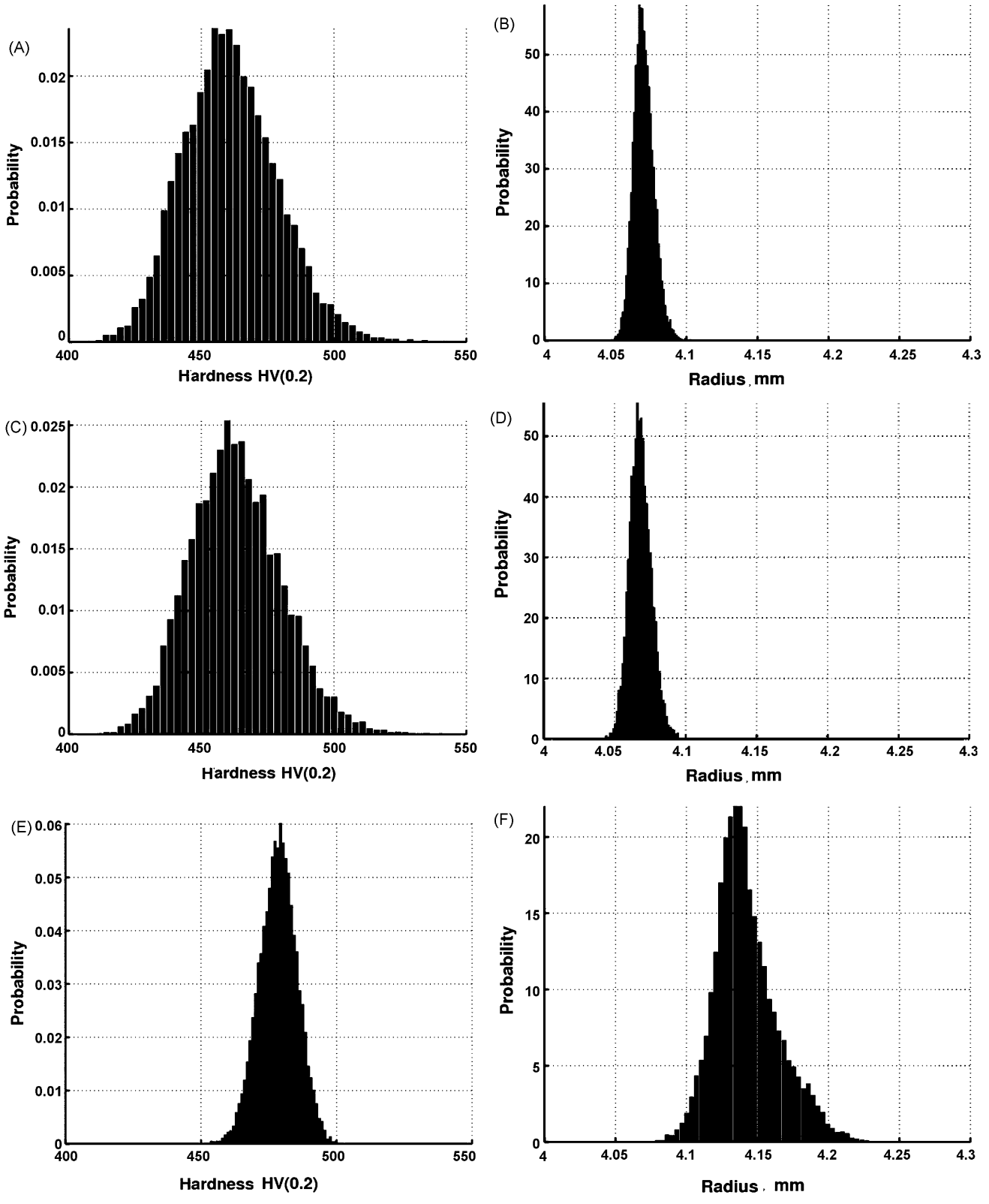

Fig. 9 – Results of the Monte Carlo analysis on the accuracy and hardness (Hv0.2) of the final product. (A) The hardness distribution after stamping, (B) The radius distribution after stamping, (C) The hardness distribution, (D) the radius distribution after stamping and waiting for 3 h stamping, (E) the hardness distribution and (F) the radius distribution after stamping, waiting and rehardening.

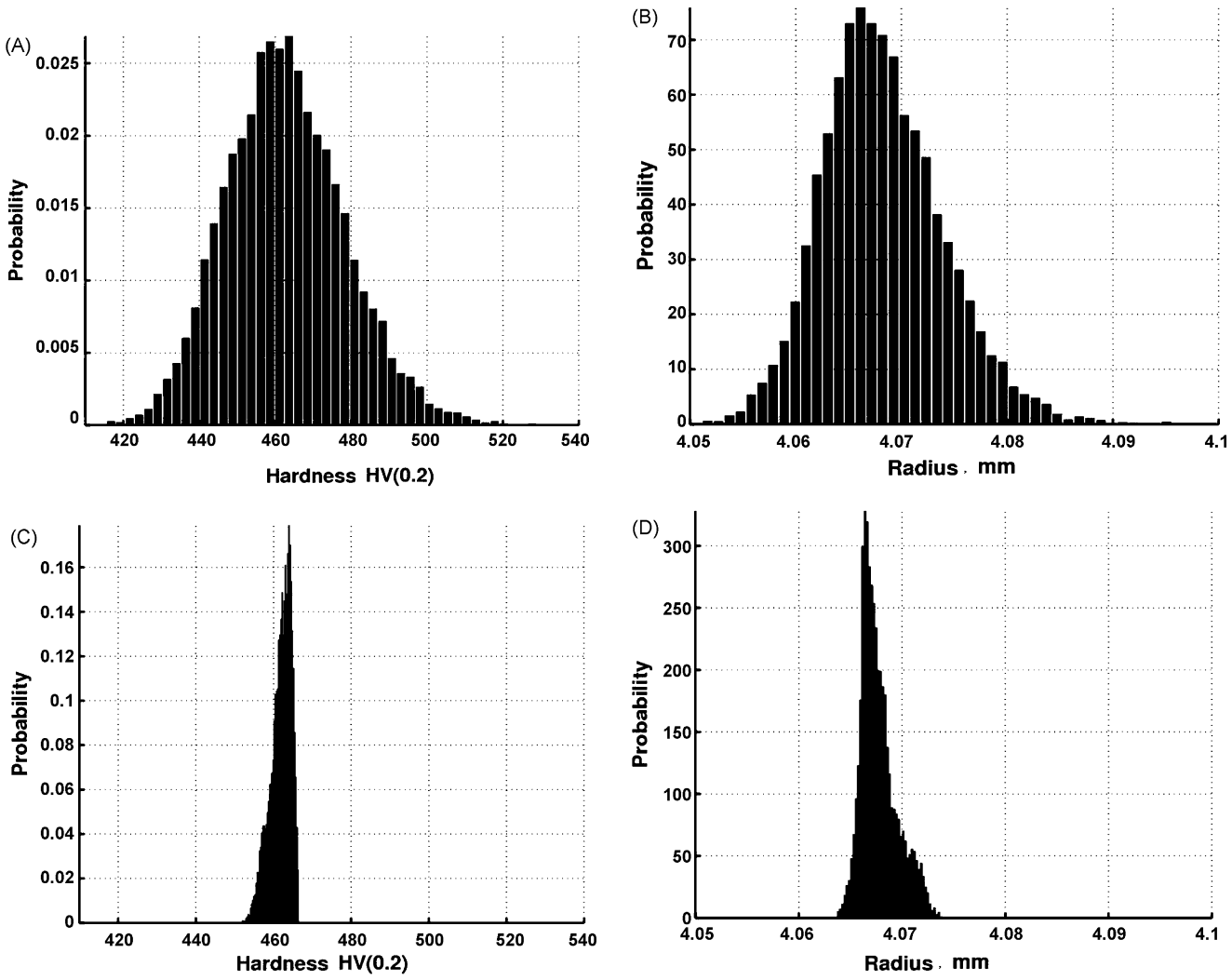

Fig. 10 – Results of Monte Carlo analysis on the influence of metal forming parameters: (A) spread of the hardness of the products, (B) spread of the radius of the products, (C) spread of the hardness due to waiting time and (D) spread of the radius due to waiting time.

the accuracy of the product. To determine where the spread in accuracy comes from, the same were carried out for the other parameters from Table 8. The Ram depths were all varied in one Monte Carlo analysis because the Ram depths depend on the accuracy of the tools. The material parameters (material thickness, chemical composition and initial flow stress) were varied together because this is the input of the material in the process. Also the temperature and the friction were varied. The results can be seen in Table 8. From this table, it can be seen that variation in the material parameters has the main influence on the deviation of the radius and the hardness.

Table 8 – Influence on the radius and hardness of different parameters by a Monte Carlo analysis

Variation on	Radius expected (mm)	Radius variation (mm)	Hardness expected (Hv0.2)	Hardness variation (Hv0.2)
All	4.0682	0.0057	462.7	14.86
Material[a]	4.0665	0.0045	465.6	14.86
Ram depth	4.0668	0.0013	465.3	0.99
Friction	4.0664	0.0024	465.4	3.32
Temperature	4.0664	0.0003	465.3	0.69
Waiting time	4.0677	0.0018	461.9	2.69

[a] Material means thickness, flow stress and Md temperature.

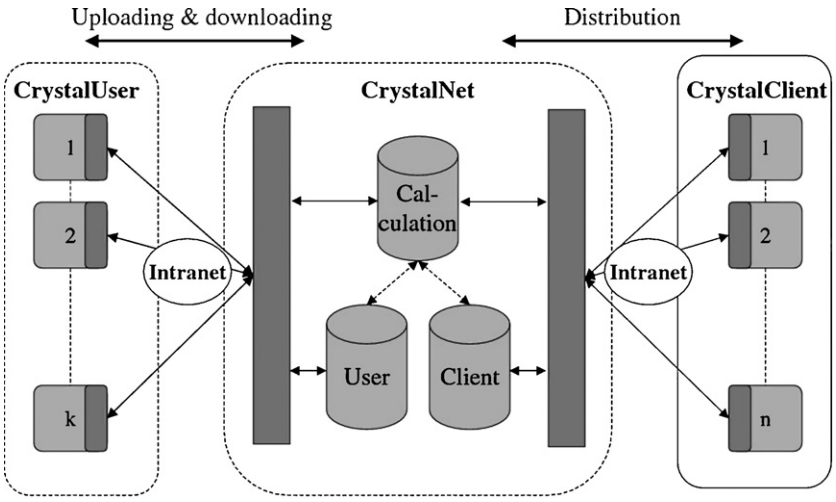

Fig. 11 – The structure of the Crystal distributive computing system. Three main components: CrystalUser, CrystalNet and CrystalClient are shown.

4.4. *Distributive computing*

4.4.1. *Introduction*

Distributed computing is based on using the idle time within computer networks, by doing defined tasks within this time period. The design choices that were made concerning the structure and the protocols to build the distributed system are based on the scalability, robustness and controllability of the system.

4.4.2. *Structure*

The distributed computing structure (Fig. 11) can be divided in three sections:

(a) crystal users (CrystalUser), these are the users of the CRYSTAL solver organized on a LAN;
(b) the server (CrystalNet), the server that is connected to the same LAN;
(c) crystal clients (CrystalClient), this are the computers on the LAN that are used for the calculations.

In general the (CrystalUser) is a subset of the (CrystalClient). The user and the server sections can be grouped to form the input–output functionality. The server and the client section form the distributing functionality. The input–output functionality is to upload FEM-calculations to the server and to download the results of the FEM-calculations from the server. The distributing functionality allows the distribution of the various calculations from the server to the clients, the computation of these calculations and returning these calculations back to the server. The entire process is monitored and controlled through the use of three databases on the server section: the user, the calculation and the client database. The user database is coupled to the calculation database and contains information about the users for instance: number of calculations uploaded and downloaded. The client database contains information about the clients such as: number of calculations done, computer architecture and calculation being computed. The client database is also coupled to the calculation database. The calculation database contains the information about the calculation such as: calculation-id, status, calculation type, calculation size and owner.

4.4.3. *Protocol*

The relatively small scale, less than thousand clients, and the reliability of the network on which this distributed computing system is to function, allow us to implement an extensive protocol to maximize controllability and robustness of the system. The most basic protocol for the distribution function to work is to allow two requests to the server. The first requests a calculation to be executed and the second requests to return the executed calculation. We have chosen to extend this basic protocol with a few announcements and requests such as: an announcement that computation is interrupted and a request to cancel current task. These extensions allow the server to anticipate on events that occur on the clients. For example in the case of the announcement that the computation is interrupted the server could react by restarting this interrupted calculation on a different client. Hence, this allows for more control over the process, an increased robustness because long calculation interruption could be averted and better process monitoring. The protocol for the input–output functionality consist of two basic requests: the first requests to upload a calculation to the server and the second requests to download results from the server. Furthermore the protocol consists of monitoring requests to determine the status of the distributed calculation.

5. Conclusions

- The DACE approach in combination with a robust solver is a powerful tool in optimising processes.
- This method can be very useful to determine the tolerances for parameters in the production process.
- The most accurate product is realized by using only the strain-induced hardening and ageing process.
- The highest hardness is realized by using the austenizing and isothermal hardening and ageing process.

- The waiting times between two steps have influence on the shape accuracy and the hardness of the product due to stress-assisted transformation. Furthermore the strain-induced transformation in the next forming stage occurs at a different temperature. This combined influence is even larger than the influence of variation in the depth of the rams. The largest influence for this product lies in the variation of material parameters. Note that this conclusion is strongly dependent on the probability distribution of the design parameters in the fourth step of the 'Compact' method.

REFERENCES

Aarts, E., Korst, J., 1989. Simulated Annealing and Boltzmann Machine. Wiley & Sons, Chichester.

Bakircioglo, H., Kocak, T., 2000. Survey of random neural network applications. European Journal of Operational Research 126, 319–330.

Barthelemy, J.-F.M., Haftka, R.T., 1993. Approximation concepts for optimum structural design—a review. Structural Optimization 5, 129–144.

Booker, A.J., Dennis, J.E., Frank, P.D., Serafini, D.B., Torczon, V., Trosset, M.W., 1999. A rigorous framework for optimization of expensive functions by surrogates. Structural Optimization 17, 1–13.

Conn, A.R., Gould, N.I.M., Toint, P.L., 2000. Trust Region Methods mps/siam Series on Optimalization, vol. 5. SIAM, Philadelphia, pp. 129–144.

Estrin, Y., 1996. In: Krausz, A.S., Krausz, K. (Eds.), Unified Constitutive Laws of Plastic Deformation. Academic Press.

Hertog den, D., Stehouwer, H.P., 2002. Optimizing color picture tubes by high-cost nonlinear programming. European Journal on Operations Research 140 (2), 197–211.

Holmquist, M., Nilsson, J.-O., Hultin, S.A., 1995. Isothermal formation of martensite in a 12Cr–9Ni–4Mo maraging stainless steel. Scripta Metallurgica et Materialia, 1367–1373.

Montgomery, D.C., 1984. Design and Analysis of Computer Experiments, 2nd ed. John Wiley & Sons, New York.

Myers, R.H., 1999. Response surface methodology—current status and future directions. Journal of Quality Technology 31, 30–43.

Narutani, T., Olson, G.B., Cohen, M., 1982. Journal de Physique 43 (12), 429.

Post, J., Beyer, J., de Vries, C., Geijselaers, H.J.M., 2001. Verification tool for 2D multi-stage metal forming processes involving small parts made of stainless steel. Shemet, 475–484.

Post, J., Datta, K., Beyer, J., 2008. Materials Science and Engineering A 485, 290–298.

Sacks, D., Welch, W.J., Mitchell, T.J., Wynn, H.P., 1989. Design and analysis of computer experiments. Statistical Science 4, 409–435.